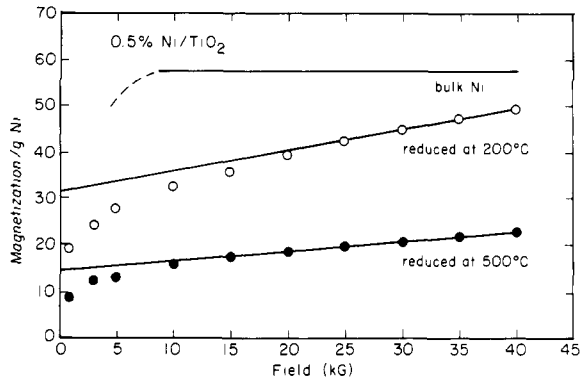

Figure 2. Magnetization vs. field for 0.5% Ni/TiO_2 reduced at 200 and 500 °C. The magnetization expected for bulk nickel is shown.

reagent grade $Ni(NO_3)_2 \cdot 6H_2O$ (Mallincroft, 99.95% pure). These samples were reduced initially in flowing hydrogen at 473 K for 20 h and then at 773 K for 1 h. Changes in the surface chemistry of the nickel were monitored by the chemisorption of hydrogen at room temperature.

The amount of hydrogen that chemisorbed at 295 K on these composites was sensitive both to the amount of nickel present and to the preparation temperature as shown in Figure 1. A suppression of hydrogen chemisorption was observed as the reduction temperature of the composite was increased from 473 to 773 K. As the nickel loading was increased, the amount of hydrogen chemisorbed became nearly independent of reduction temperature as expected for bulk nickel. The trends in chemisorption observed for the lower nickel loadings are due to two effects: (1) interactions of the nickel with the TiO_2 and (2) changes in the dispersion of the nickel. We present here magnetic studies on the 0.5% Ni/TiO_2 sample which show that the large changes in chemisorption as a function of reduction temperature are due to a strong interaction between nickel and TiO_2.

Magnetization vs. field was measured for these samples with a SHE SQUID magnetometer at 5 K in fields from 1 to 40 kG. Figure 2 shows the magnetization per gram of nickel vs. field for 0.5% Ni/TiO_2 reduced at 473 and 773 K. Extrapolation of the data for fields greater than 30 kG to zero gives the saturation magnetization M_s(473 K) = 31.7 per g of Ni for the sample reduced at 473 K and M_s(773 K) = 14.8 per g of Ni for the sample reduced at 773 K. M_s(473 K) is 55% of the value expected if all the nickel were present as bulk nickel, indicating that some unreduced NiO remains. A temperature of 773 K is high enough to reduce all the NiO to Ni[8] and therefore M_s should increase to the value observed for bulk nickel. The fact that M_s(773 K) is less than M_s(473 K), however, suggests that much of the nickel (~75%) is not present as bulk nickel. Furthermore, since this loss of bulk nickel after the high-temperature reduction correlates well with the suppression of hydrogen chemisorption we conclude that the change in chemisorption properties is associated with the change in the form of nickel present in the system.

The slope of the magnetization vs. field curves for fields greater than 30 kG shows that the samples contain localized, unpaired electrons. Since the TiO_2 starting material is temperature independent and diamagnetic down to 5 K, this result suggests that part of the TiO_2 has been reduced. Although the analysis is complicated by the exchange field of the ferromagnetic nickel, the magnitude of the moment indicates that ~5% of the Ti^{4+} in the support has been reduced to Ti^{3+}. We have obtained electron spin resonance spectra of these materials and the presence of a resonance due to Ti^{3+} supports this conclusion. This reduced titanium oxide is present after reduction at both 473 and 773 K.

In summary, we have shown that for 0.5% Ni/TiO_2 reduced at 773 K, a large fraction of the nickel is not present as bulk nickel. Furthermore, a significant fraction of the support is present as paramagnetic reduced titanium oxide, TiO_x (where $x < 2$), after reduction at both 473 and 773 K. We conclude that the changes in chemisorption properties for samples reduced at 773 K are due to a change in the electronic structure of the material and not just a change in the number of metal sites exposed for chemisorption. To account for the loss of bulk nickel at the 773 K reduction temperature, we propose the formation of a metastable Ni–Ti–O phase. To substantiate the presence of such a composite and to determine its properties, we have begun electron spin resonance studies of the Ni/TiO_2 system and are beginning magnetic studies on other metal/TiO_2 systems.

Acknowledgment. This research was supported by a Presidential Young Investigator Award from the National Science Foundation (Grant CHE83-51881) and matching funds from E.I. du Pont de Nemours and Co.

Registry No. TiO_2, 13463-67-7; Ni, 7440-02-0.

(8) Robertson, S. D.; McNicol, B. D.; DeBaas, J. H.; Kloet, S. C.; Jenkins, J. W. *J. Catal.* **1975**, *37*, 424.

Synthesis, Structure, and Magnetic Properties of an Asymmetric μ_3-Oxotriiron(III) Complex: A New Type of $\{Fe_3O\}^{7+}$ Core

Sergiu M. Gorun and Stephen J. Lippard*

Department of Chemistry
Massachusetts Institute of Technology
Cambridge, Massachusetts 02139
Received March 14, 1985

Polynuclear iron oxo complexes have interested inorganic and biological chemists for many years.[1-3] Recently μ-oxodiiron(III) complexes having properties comparable to those of the met forms of hemerythrin, a marine invertebrate oxygen transport protein, were prepared and characterized.[4] Further studies led to the synthesis of hydroxo- and phosphodiester-bridged analogues,[5,6] the latter being of likely relevance to several biologically occurring iron–phosphate systems.[7] Binuclear oxo-bridged iron centers have also been suggested to be important for initiating the formation of the polynuclear iron core in the iron storage protein ferritin.[7d,e] We were therefore interested to investigate whether larger iron–oxo aggregates might be constructed by controlled oligomerization in a nonaqueous solvent from $\{Fe_2O\}^{4+}$ and Fe^{3+} building blocks, as illustrated for example by eq 1 and 2. It is of value to compare

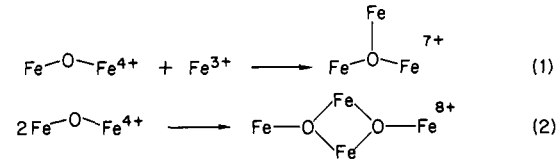

properties of the resulting polynuclear iron oxo complexes with those of ferritin, the polynuclear iron core of which has been postulated[7a,8] to be comprised of such units. As described in the

(1) Welo, L. A. *Phil. Mag. S7* **1928**, *6*, 481–509.
(2) Spiro, T. G.; Saltman, P. *Struct. Bonding (Berlin)* **1969**, *6*, 115–156.
(3) Gray, H. B.; Schugar, H. J. In "Inorganic Biochemistry"; Eichhorn, G., Ed.; American Elsevier: New York, 1973; pp 102–118.
(4) (a) Armstrong, W. H.; Lippard, S. J. *J. Am. Chem. Soc.* **1983**, *105*, 4837–4838. (b) Wieghardt, K.; Pohl, K.; Gebert, W. *Angew. Chem., Int. Ed. Engl.* **1983**, *22*, 727. (c) Armstrong, W. H.; Spool, A.; Papaefthymiou, G. C.; Frankel, R. B.; Lippard, S. J. *J. Am. Chem. Soc.* **1984**, *106*, 3653–3667. (d) Spool, A.; Williams, I. D.; Lippard, S. J. *Inorg. Chem.*, in press.
(5) Armstrong, W. H.; Lippard, S. J. *J. Am. Chem. Soc.* **1984**, *106*, 4632–4633.
(6) Armstrong, W. H.; Lippard, S. J. *J. Am. Chem. Soc.* **1985**, *107*, 3730–3731.
(7) (a) Theil, E. C. *Adv. Inorg. Biochem.* **1983**, *5*, 1–38. (b) Antanaitis, B. C.; Aisen, P. *Adv. Inorg. Biochem.* **1983**, *5*, 111–136. (c) Taborsky, G. *Adv. Inorg. Biochem.* **1983**, *5*, 235–279. (d) Mansour, A. N.; Thompson, C.; Theil, E. C.; Chasteen, N. D.; Sayers, D. E. *J. Biol. Chem.*, in press. (e) Chasteen, N. D.; Antanaitis, B. C.; Aisen, P. *J. Biol. Chem.* **1985**, *260*, 2926–2929.
(8) Heald, S. M.; Stern, E. A.; Bunker, B.; Holt, E. M.; Holt, S. J. *J. Am. Chem. Soc.* **1979**, *101*, 67–73.

0002-7863/85/1507-4568$01.50/0

present and forthcoming[9] papers, we have achieved both reactions 1 and 2 using polyimidazolyl alkoxide or polypyrazolylborate (reaction 2 only) as well as bridging carboxylate ligands. Here we describe the asymmetric μ_3-oxotriiron(III) complex $[Fe_3O(TIEO)_2(O_2CPh)_2Cl_3]$ (**1**), assembled by the route given in eq 1 and employing the new ligand 1,1,2-tris(1-methylimidazol-2-yl)ethoxide ($TIEO^-$).

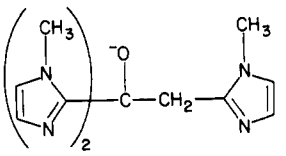

Compound **1** was prepared in the following manner. To a rapidly stirred solution containing 0.202 g (0.336 mmol) of $(Et_4N)_2[Fe_2OCl_6]$[10] in 10 mL of CH_3CN were added 0.110 g (0.335 mmol) of $(Et_4N)[FeCl_4]$[11] and, after 5 min, 0.097 g (0.67 mmol) of anhydrous sodium benzoate. After 1 h a solution containing 0.195 g (0.68 mmol) of TIEOH[12] and 0.2 mL (1.4 mmol) of dry Et_3N dissolved in 15 mL of CH_3CN was added dropwise over a 5-min period to the brown suspension. The color changed to deep red-brown. After 30 min a white solid was filtered off and the solvent was removed in vacuo. Several successive additions and removals of acetonitrile allowed the separation of more white solid. Recrystallization of the colored material from acetonitrile/benzene afforded **1** as a yellow microcrystalline solvate ($\mathbf{1}\cdot 2C_6H_6$) in 63% yield.[13] X-ray quality crystals were obtained by slow diffusion of benzene into an acetonitrile solution of **1** over a period of 3–4 weeks.

The structure of $\mathbf{1}\cdot 2C_6H_6$, determined by single-crystal X-ray diffraction methods,[14] contains discrete μ_3-oxotriiron(III) complexes shown in Figure 1. Unlike the symmetric μ_3-oxotriiron(III) center in the basic metal carboxylates,[15] the $\{Fe_3O\}^{7+}$ core in **1** consists of an isosceles triangle of iron atoms with the metrical parameters given in Figure 1. The equivalent Fe1---Fe3 and Fe2---Fe3 sides of the triangle are each bridged by an alkoxide oxygen atom of the $TIEO^-$ ligand and by a bidentate benzoate group. Iron atoms Fe1 and Fe2 are also coordinated to two imidazole ring nitrogen atoms, and all three iron atoms have a terminal chloride ligand. The third imidazole ring of each $TIEO^-$ ligand is not bound to iron; the same type of tridendate N,N,O coordination of $TIEO^-$ to iron(III) is encountered in the structure of the mononuclear $[Fe(TIEO)_2]^+$ complex.[12] Other features of the geometry are typical for high-spin iron(III).[16]

Solid-state magnetic susceptibility data were collected by using a SQUID-type susceptometer between 2.5 and 298 K. Magnetic saturation studies at 2.5 and 3.8 K revealed the ground state to

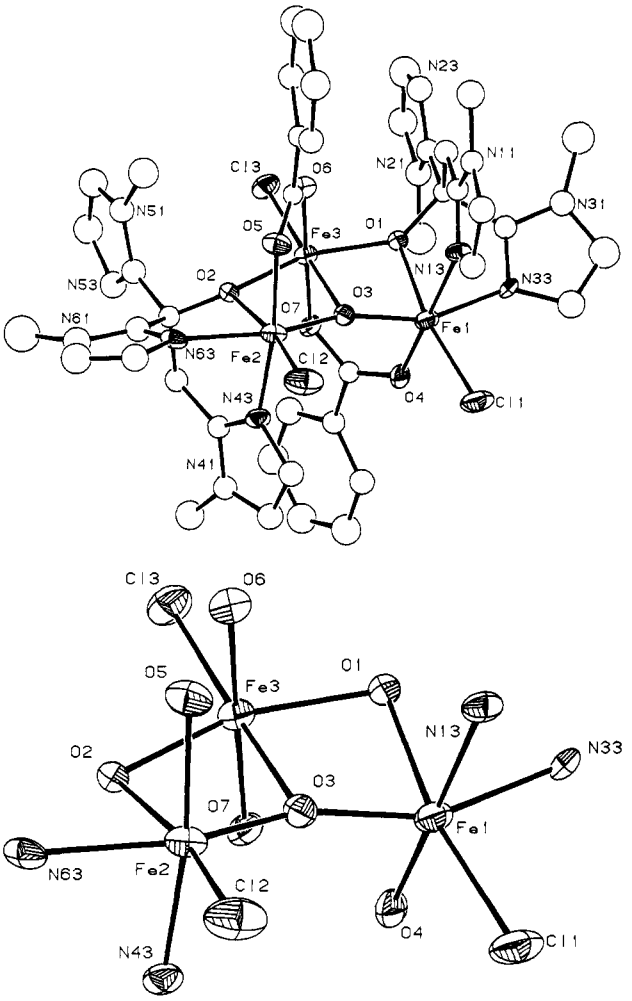

Figure 1. Structure (top) of $[Fe_3(TIEO)_2(O_2CPh)_2Cl_3]$ (**1**), showing the 40% probability thermal ellipsoids and labels for all non-hydrogen atoms except carbon. Selected bond lengths (Å) and angles (deg) are as follows: Fe1–O3, 1.862 (7); Fe2–O3, 1.867 (7); Fe3–O3, 2.067 (6); Fe1---Fe2, 3.667 (1); Fe1---Fe3, 3.018 (2); Fe2---Fe3, 3.027 (2); Fe1–O1, 2.074 (6); Fe3–O1, 1.994 (6); Fe2–O2, 2.074 (6); Fe3–O2, 1.991 (6); Fe1–O4, 2.062 (7); Fe3–O7, 2.034 (6); Fe2–O5, 2.080 (7); Fe3–O6, 2.057 (6); Fe1–N33, 2.155 (8); Fe1–N13, 2.142 (8); Fe2–N63, 2.169 (9); Fe2–N43, 2.117 (8); Fe1–Cl1, 2.283 (3); Fe2–Cl2, 2.282 (3); Fe3–Cl3, 2.264 (3); Fe1–O3–Fe2, 159.1 (5); Fe1–O3–Fe3, 100.3 (3); Fe2–O3–Fe3, 100.5 (3); Fe1–O1–Fe3, 95.8 (3); Fe2–O2–Fe3, 96.2 (3). The coordination geometry of the three iron atoms is depicted at the bottom.

have $S = {}^5/_2$, which differs from that of the basic iron carboxylates, $[Fe_3O(O_2CR)_6]^+$, symmetric μ_3-oxotriiron(III) complexes having a $S = {}^1/_2$ ground state.[17] The temperature dependence of the magnetic susceptibility was analyzed by assuming isotropic exchange with the spin Hamiltonian

$$\mathcal{H} = -2\sum_{i,j=1}^{3} J_{ij}\vec{S}_i\cdot\vec{S}_j; \quad S_{i,j} = {}^5/_2$$

no intercluster interaction, and zero TIP. Two superexchange pathways were allowed, the coupling constants for which refined nicely to $J_{12} = -55.0$ (6) cm^{-1} and $J_{13} = J_{23} = -8.0$ (4) cm^{-1}, revealing antiferromagnetic behavior. At 290 K the effective magnetic moment is 6.50 μ_B, or 3.75 μ_B per iron atom. The inequality $|J_{12}| > |J_{13}|$ is the one expected from the relative iron(III)–oxo bond lengths, Fe1–O3 = Fe2–O3 < Fe3–O3.[12,16] The value of $|J_{12}|$ is unprecedented among structurally characterized iron(III)–oxo complexes, being larger than the magnitude of the antiferromagnetic coupling constants found for basic iron carboxylates, ~30 cm^{-1},[18] but less than the 80–130-cm^{-1} values

(9) Gorun, S.; Armstrong, W. H.; Lippard, S. J., manuscript in preparation.

(10) Armstrong, W. H.; Lippard, S. J. *Inorg. Chem.* **1985**, *24*, 981–982.

(11) Prepared from $FeCl_3\cdot 6H_2O$ and Et_4NCl by a method similar to the one employed for the iron(II) analogue: Gill, N. S.; Taylor, F. B. *Inorg. Synth.* **1967**, *9*, 136–142.

(12) Gorun, S.; Lippard, S. J., manuscript in preparation.

(13) Elemental analysis: Calcd for $Fe_3Cl_3O_7N_{12}C_{54}H_{56}$ ($\mathbf{1}\cdot 2C_6H_6$): C, 51.52; H, 4.48; N, 13.35; Cl, 8.45. Found: C, 51.69; H, 4.58; N, 13.32; Cl, 8.51.

(14) X-ray analysis: The compound $[Fe_3O(TIEO)_2(O_2CPh)_2Cl_3]\cdot 2C_6H_6$ crystallizes in the triclinic system, space group $P\bar{1}$, with a = 14.080 (1) Å, b = 15.879 (2) Å, c = 14.043 (2) Å, α = 92.50 (1)°, β = 100.296 (8)°, γ = 67.095 (7)°, V = 2844.4 Å^3, ρ_{obsd} = 1.46 (1) g cm^{-3}, ρ_{calcd} = 1.470 g cm^{-3}, Z = 2. With the use of 2692 unique reflections ($F_o > 4\sigma(F_o)$) collected at 20 °C with Mo K$\bar{\alpha}$ (λ = 0.7107 Å) radiation out to 2θ = 44° the structure was solved by direct and difference Fourier methods and refined using 375 variables to a current value for the discrepancy index R_1 of 0.049. Atomic positional and thermal parameters are provided as supplementary material. Full details will be reported elsewhere.

(15) (a) Cotton, F. A.; Wilkinson, G. "Advanced Inorganic Chemistry"; Wiley: New York, 1980; pp 154–155. (b) Catterick, J.; Thornton, P. *Adv. Inorg. Chem. Radiochem.* **1977**, *20*, 291–362.

(16) (a) Murray, K. S. *Coord. Chem. Rev.* **1974**, *12*, 1–35. (b) Anderson, B. F.; Webb, J.; Buckingham, D. A.; Robertson, G. B. *J. Inorg. Biochem.* **1982**, *16*, 21–32. (c) Sinn, E.; Sim, G.; Dose, E. V.; Tweedle, M. F.; Wilson, L. F. *J. Am. Chem. Soc.* **1978**, *100*, 3375–3390. (d) Thich, J. A.; Toby, B. H.; Powers, D. A.; Potenza, J. A.; Schugar, H. J. *Inorg. Chem.* **1981**, *20*, 3314–3317.

(17) Abragam, A.; Horowitz, J.; Yuou, J. *J. Phys. Radium* **1952**, *13*, 489–490.

observed for the $\{Fe_2O\}^{4+}$, $\{Fe_2O(O_2CR)_2\}^{2+}$, and $\{Fe_2O(O_2P(OR)_2)_2\}^{2+}$ cores.[4,6,16]

In conclusion, the novel asymmetric $\{Fe_3O\}^{7+}$ core has been synthesized by the route given in eq 1. The resulting isosceles triangle of iron atoms has antiferromagnetic exchange and ground-state magnetic properties quite different from those of the extensively studied basic iron carboxylates.[15,18] These results provide valuable insight into the relationships that occur between magnetic and structural properties of polynuclear iron-oxo complexes and should facilitate the study of such units in biological systems such as ferritin.

Acknowledgment. This work was supported by National Institutes of Health Grant GM-32134 from the National Institute of General Medical Sciences. Magnetic measurements and some computations were made at the SQUID magnetometer facility of the Francis Bitter National Magnet Laboratory. We thank Drs. R. B. Frankel and G. C. Papaefthymiou for helpful discussions and Drs. E. C. Theil and N. D. Chasteen for preprints of articles describing their work.

Registry No. $1 \cdot 2C_6H_6$, 96998-70-8.

Supplementary Material Available: Atomic positional and thermal parameters for compound $1 \cdot 2C_6H_6$ (2 pages). Ordering information is given on any current masthead page.

(18) Dziobkowski, C. T.; Wrobleski, J. T.; Brown, D. B. *Inorg. Chem.* **1981**, *20*, 671-678 and references cited therein.

Cleavage of Ruthenium and Osmium Porphyrin Dimers: Formation of Organometallic Ruthenium Porphyrin Complexes and Highly Reduced Metalloporphyrin Species

J. P. Collman,* P. J. Brothers, L. McElwee-White, E. Rose, and L. J. Wright

Department of Chemistry, Stanford University Stanford, California 94305

Received January 29, 1985

Early reports on naturally occurring and synthetic metalloporphyrins focused on heteroatom donors (N, P, O, S) or CO coordinated to the metal. More recently, a small number of metalloporphyrin complexes containing metal-carbon bonds in the axial coordination sites have been reported. These include alkyl, acyl, carbene, vinyl, vinylidene, and acetylene species. Hydride complexes have also been prepared.[1]

We recently described the characterization of the double-bonded porphyrin dimers $[M(Por)]_2$ (M = Ru, Os; Por = OEP, TTP).[2,3] In the presence of any potentially coordinating ligand, these dimers are cleaved to form $M(Por)L_2$ species. Formation of the complexes $Ru(TTP)L_2$ (L = py, **1**; THF, **2**; CO, **3**) is illustrated in Scheme I. Preparations of these products by independent routes have been described in the literature.[4-7]

Scheme I

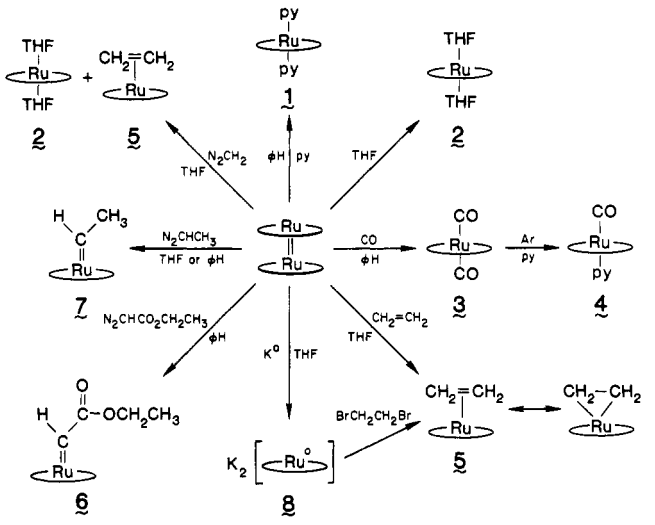

Treatment of a THF solution of $[Ru(Por)]_2$ (Por = OEP, TTP) with ethylene (5 min at room temperature), followed by purging with Ar and recrystallization from THF/ROH (R = C_2H_5, $CH(CH_3)_2$) yields the novel organometallic metalloporphyrin ethylene complex $Ru(Por)(CH_2{=}CH_2)$.[8] The coordinated ethylene in $Ru(TTP)(CH_2{=}CH_2)$ (**5**) gives rise to a singlet at -4.06 ppm in the ^1H NMR spectrum. The integrated intensities indicate that there is one ethylene present per Ru porphyrin moiety. The upfield shift of 9 ppm (relative to free ethylene) can be attributed to the porphyrin ring current effect. The ^1H NMR spectrum remains unchanged at -85 °C. In the presence of ethylene, no coordinated olefin is observed by ^1H NMR indicating fast exchange on the NMR time scale. We are currently investigating the reaction of the dimers with other olefins.

The ease with which the ruthenium dimer can be cleaved upon treatment with neutral donor ligands suggested that reaction with a neutral carbene precursor ":CRR'" might lead to carbene complexes of the form Ru(Por)(CRR'). A vinylidene complex, $Ru(TPP)(C{=}C(p\text{-}C_6H_4Cl)_2)$, had been prepared by insertion of Ru into a free base porphyrin already containing the carbene moiety bridged between two pyrrole nitrogen atoms.[1g]

(1) (a) Abeysekera, A. M.; Grigg, R.; Trocha-Grimshaw, J.; Viswanatha, V. *J. Chem. Soc., Perkin Trans. 1* **1977**, 36-44. (b) Abeysekera, A. M.; Grigg, R.; Trocha-Grimshaw, J.; Viswanatha, V. *J. Chem. Soc., Perkin Trans. 1* **1977**, 1395-1403. (c) Ogoshi, H.; Setsune, J.; Yoshida, Z. *J. Am. Chem. Soc.* **1977**, *99*, 3869-3870. (d) Ogoshi, H.; Setsune, J.-I.; Nanbo, Y.; Yoshida, Z.-I. *J. Organomet. Chem.* **1978**, *159*, 329-339. (e) Wayland, B. B.; Woods, B. A.; Pierce, R. *J. Am. Chem. Soc.* **1982**, *104*, 302-303. (f) De Cian, A.; Colin, J.; Schappacher, M.; Ricard, L.; Weiss, R. *J. Am. Chem. Soc.* **1981**, *103*, 1850-1851. (g) Chan, Y. W.; Renner, M. W.; Balch, A. L. *Organometallics* **1983**, *2*, 1888-1889. (h) Mansuy, D. *Pure Appl. Chem.* **1980**, *52*, 681-690.

(2) (a) Collman, J. P.; Barnes, C. E.; Swepston, P. N.; Ibers, J. A. *J. Am. Chem. Soc.* **1984**, *106*, 3500-3510. (b) Collman, J. P.; Barnes, C. E.; Woo, L. K. *Proc. Natl. Acad. Sci. U.S.A.* **1983**, *80*, 7684-7688.

(3) Abbreviations: Por = porphyrinato dianion unspecified; OEP = 2,3,7,8,12,13,17,18-octaethylporphyrinato dianion; TPP = 5,10,15,20-tetraphenylporphyrinato dianion; TTP = 5,10,15,20-tetra-*p*-tolylporphyrinato dianion; py = pyridine; THF = tetrahydrofuran.

(4) (a) Antipas, A.; Buchler, J. W.; Gouterman, M.; Smith, P. D. *J. Am. Chem. Soc.* **1978**, *100*, 3015-3024. (b) Collman, J. P.; Barnes, C. E.; Collins, T. J.; Brothers, P. J.; Gallucci, J.; Ibers, J. A. *J. Am. Chem. Soc.* **1981**, *103*, 7030-7032.

(5) Collman, J. P.; Barnes, C. E.; Brothers, P. J.; Collins, T. J.; Ozawa, T.; Gallucci, J. C.; Ibers, J. A. *J. Am. Chem. Soc.* **1984**, *106*, 5151-5163. $Ru(TTP)(THF)_2$ NMR (THF-d_8, 300 MHz) H_β 8.17 (s), H_o, H_m 7.94 (d), 7.49 (d), CH_3 2.63 (s) ppm. $Ru(OEP)(THF)_2$ NMR (THF-d_8, 300 MHz) H_{meso} 9.29 (s), CH_2CH_3 3.87 (q), CH_2CH_3 1.83 (t) ppm.

(6) Eaton, G. R.; Eaton, S. S. *J. Am. Chem. Soc.* **1975**, *97*, 235-236. $Ru(TTP)(CO)_2$ NMR (C_6D_6, 300 MHz) H_β 9.05 (s), H_o, H_m 8.08 (d), 7.24 (d), CH_3 2.39 (s) ppm. The complex was identified by IR and NMR spectroscopy in the presence of excess CO.

(7) Little, R. G.; Ibers, J. A. *J. Am. Chem. Soc.* **1973**, *95*, 8583-8590.

(8) (a) The ethylene complex can be formulated either as a Ru(IV) metallocyclopropane or as a Ru(II) ethylene π complex. We use the latter formulation. $Ru(TTP)(CH_2{=}CH_2)$ NMR (THF-d_8, 300 MHz) H_β 8.37 (s), H_o, H_m 7.95 (d), 7.49 (br d), CH_3 2.64 (s), CH_2CH_2 -4.06 (s) ppm; NMR (C_6D_6, 300 MHz) H_β 8.81 (s), H_o, $H_{o'}$, H_m, $H_{m'}$ 8.19 (d), 8.04 (d), 7.30 (d), 7.25 (d), CH_3 2.39 (s), CH_2CH_2 -3.54 (s) ppm; MS (DEI), m/z $[M]^+$ 798; $[M - CH_2CH_2]^+$ (base peak) 770; UV-vis (THF) λ_{max} (log ϵ), 408 (5.23), 504 (4.21), 524 (sh) nm. Anal. Satisfactory C, H, N for $Ru(TTP)(CH_2{=}CH_2)\cdot THF$. One equivalent of THF observed by ^1H NMR in C_6D_6. $Ru(OEP)(CH_2{=}CH_2)$ NMR (THF-d_8, 300 MHz) H_{meso} 9.63 (s), CH_2CH_3 3.94 (q), CH_2CH_3 1.84 (t), CH_2CH_2 -4.78 (s) ppm; MS (NDCI), m/z $[M]^-$ (base peak) 662; $[M - CH_2CH_2]^-$ 634; UV-vis (THF) λ_{max} (log ϵ), 388 (5.12), 497 (sh), 520 (4.28), 543 (sh) nm. (b) A complex claimed on the basis of an electronic spectrum to be a ruthenium OEP ethylene complex is mentioned in the secondary literature. However, this species was neither isolated nor characterized. James, B. R.; Addison, A. W.; Cairns, M.; Dolphin, D.; Farrell, N. P.; Paulson, D. R.; Walker, S. *Fundam. Res. Homogeneous Catal.* **1979**, *3*, 751-772.

0002-7863/85/1507-4570$01.50/0